methacrylate as a comonomer. The copolymer **1** was shown to have good film-forming properties on a solid substrate. The fluorescence of the polymer was effectively quenched by photochemically generated acid and afforded finely resolved fluorescent images on a solid substrate.

Experimental Section

4: Potassium carbonate (82.9 g, 0.60 mol) and benzyl bromide (136.8 g, 0.80 mol) were added to a solution of 5-fluoro-2-nitrophenol (**3**) (94.3 g, 0.60 mol) in DMF (200 mL). The resulting mixture was stirred at 100 °C for 3 h, filtered, and the filtrate diluted with diethyl ether. The organic layer was washed with water and dried with anhydrous magnesium sulfate. Concentration, followed by vacuum distillation (142–146 °C, 0.1 Torr) of the residue gave **4** (123.1 g, 83 %) as a yellow solid. M.p. 55–56 °C; ^{1}H NMR (200 MHz, $CDCl_3$): $\delta = 5.18$ (s, 2H), 6.66–6.87 (m, 2H), 7.32–7.49 (m, 5H), 7.94 (d, 1H); elemental analysis calcd (%) for $C_{13}H_{10}N_1O_3F_1$ (247.23): C 63.16, H 4.08, N 5.67; found: C 63.50, H 4.09, N 5.21.

5: Potassium carbonate (51.83 g, 0.38 mol) was added to a solution of **4** (123.1 g, 0.50 mol) and 2-(methylamino)ethanol (56.3 g, 0.75 mol) in DMF (200 mL). The resulting mixture was heated at 100 °C for 3 h and poured into water (1 L). The yellow precipitate was collected, dried, and dissolved in THF. Precipitation into hexane provided **5** (128.4 g, 85.3 %). M.p. 104–106 °C; ^{1}H NMR (200 MHz, $CDCl_3$): $\delta = 2.41$ (s, 1H), 3.03 (s, 3H), 3.50 (t, 2H), 3.77 (t, 2H), 5.13 (s, 2H), 6.10–6.22 (m, 2H), 7.27–7.50 (m, 5H), 7.88 (d, 1H); elemental analysis calcd (%) for $C_{16}H_{18}N_2O_4$: (302.33): C 63.57, H 6.00, N 9.27; found: C 63.50, H 6.09, N 9.21.

7: A mixture of **5** (24.2 g, 0.08 mol) and 10 % Pd/C (3.9 g) in THF (200 mL) was stirred under hydrogen at 25 °C for 12 h. The catalyst was removed by filtration, and 4-pyridinecarboxaldehyde (8.57 g, 0.08 mmol) was added to the filtrate. The resulting solution was stirred at 25 °C for 3 h. Lead(IV) acetate (44.38 g, 0.10 mol) was slowly added to the solution and the mixture stirred vigorously at 25 °C for 3 h. Removal of lead diacetate followed by flash column chromatography (silica gel, THF) gave **7** (17.14 g, 80.0 %) as a yellow solid. M.p. 178–180 °C; ^{1}H NMR (200 MHz, $[D_6]$DMSO): $\delta = 3.03$ (s, 3H), 3.34–3.63 (m, 4H), 4.72 (t, 1H), 6.88 (d, 1H), 7.01(s, 1H), 7.51 (d, 1H), 7.97 (d, 2H), 8.78 (d, 2H); elemental analysis calcd (%) for $C_{15}H_{15}N_3O_2$ (269.30): C 66.9, H 5.61, N 15.60; found: C 66.1, H 5.69, N 15.41.

8: The benzoxazole intermediate **7** (4.80 g, 17.84 mmol) was dissolved in dichloromethane (200 mL) and methacryloyl chloride (3.73 g, 35.68 mmol) and TEA (6.0 mL, 43.11 mmol) were added. The mixture was stirred at 25 °C for 12 h, poured into water, and extracted with dichloromethane. The organic layer was concentrated in vacuo, and silica gel column chromatography (25 % EtOAC/hexane) afforded **8** (4.47 g, 74.4 %). M.p. 60–62 °C; λ_{max} ($CHCl_3$) = 378 nm; ^{1}H NMR (200 MHz, $CDCl_3$): $\delta = 1.90$ (s, 3H), 3.07 (s, 3H), 3.73 (t, 2H), 4.36 (t, 2H), 5.53 (s, 1H), 6.05 (s, 1H), 6.82–6.87 (m, 2H), 7.60 (d, 1H), 7.99 (d, 2H) 8.74 (d, 2H); elemental analysis calcd (%) for $C_{19}H_{19}N_3O_3$ (327.38): C 67.64, H 5.68, N 12.45; found: C 67.9, H 5.74, N 12.2.

Copolymer 1 P(4PBZMA/MMA): A solution containing monomer **8** (0.50 g, 1.48 mmol), MMA (0.15 g, 1.49 mmol), AIBN (9.7 mg) and NMP (2.5 mL) in an ampoule was subjected to repeated freeze–thaw cycles before the ampoule was sealed under vacuum. The sealed ampoule was heated at 65 °C for 40 h. After polymerization, the product was precipitated into methanol and dried to give **1** (0.385 g, 59.2 %) as a yellow powder.

Received: November 29, 1999
Revised: February 24, 2000 [Z14327]

---

[1] A. M. Vekselman, C. Zhang, G. D. Darling, *Chem. Mater.* **1997**, *9*, 1942.
[2] C. Zhang, A. M. Vekselman, G. D. Darling, *Chem. Mater.* **1995**, *7*, 850.
[3] M. Schilling, H. E. Katz, F. M. Houlihan, J. M. Kometani, S. M. Stein, O. Nalamasu, *Macromolecules* **1995**, *28*, 110.
[4] J.-M. Kim, J.-H. Kang, D. K. Han, C.-W. Lee, K.-D. Ahn, *Chem. Mater.* **1998**, *10*, 2332.
[5] J.-M. Kim, T.-E. Chang, J.-H. Kang, D. K. Han, K.-D. Ahn, *Adv. Mater.* **1999**, *11*, 1499.
[6] K. H. Park, K. M. Yean, M. Y. Lee, S.-D. Lee, D.-H. Shin, C. J. Lee, N. Kim, *Polymer* **1998**, *39*, 7061.
[7] E. Reichmanis, F. M. Houlihan, O. Nalamasu, T. X. Neenan, *Chem. Mater.* **1991**, *3*, 394.
[8] S. A. Macdonald, C. G. Willson, J. M. J. Fréchet, *Acc. Chem. Res.* **1994**, *27*, 151.
[9] Q. J. Niu, J. M. J. Fréchet, *Angew. Chem.* **1998**, *110*, 685; *Angew. Chem. Int. Ed.* **1998**, *37*, 667.
[10] C.-M. Chung, K.-D. Ahn, *React. Func. Polym.* **1999**, *40*, 1.

Halogen Bonding versus Hydrogen Bonding in Driving Self-Assembly Processes[**]

Eleonora Corradi, Stefano V. Meille, Maria T. Messina, Pierangelo Metrangolo,[*] and Giuseppe Resnati[*]

It is well known[1] that carbon-bound halogen atoms (frequently iodine and bromine, but also chlorine and even fluorine) can act as electron acceptors and form short contacts with different species (both neutral and negatively charged) that possess an ability to act as an electron donor.[2] These noncovalent interactions can be strong enough to control the aggregation of organic molecules in solid,[3] liquid,[4] and gas[5, 6] phases and the term "halogen bonding"[2, 6] has been suggested in order to emphasize the similarity with hydrogen bonding. While metal-ion coordination[7] is frequently the key feature in inorganic supramolecular systems, hydrogen bonding[8] is by far the most frequently used tool to assemble organic molecules in solid, liquid, or gas phases, and it plays an important role in stabilizing supramolecular aggregates even in water.

Here we show that when the recognition pattern controlling the self-assembly process can be based on either hydrogen or halogen bonding, the latter can dominate over the former and, under appropriate conditions, will single out the molecules that will be involved in the construction of supramolecular architectures. We have already described specific I···N intermolecular interactions occurring between α,ω-diiodoperfluoroalkanes and dinitrogen hydrocarbons.[9–11] These interactions are strong enough to overcome the low affinity[12] that exists between perfluorocarbons and hydrocarbons to assemble them into oligomeric structures in the liquid phase[4] and into crystalline 1D networks in the solid phase.[9–11]

---

[*] Dr. P. Metrangolo, Prof. Dr. G. Resnati, Dr. E. Corradi,
Prof. Dr. S. V. Meille, Dr. M. T. Messina
Dipartimento di Chimica
Politecnico di Milano
7, via Mancinelli, 20131 Milano (Italy)
Fax: (+39) 02-2399-3080
E-mail: resnati@dept.chem.polimi.it

[**] Perfluorocarbon–hydrocarbon self-assembly, part IX. This work was supported by MURST (Cofinanziamento '99) and EU (COST-D12-0012). We thank Dr. A. Lunghi and Dr. P. Cardillo (Stazione Sperimentale Combustibili, S. Donato Milanese, Italy) for ARC experiments. Part VIII: ref. [9].

Supporting information for this article is available on the WWW under http://www.wiley-vch.de/home/angewandte/ or from the authors.

The ability of halogen bonding to force perfluorocarbons and hydrocarbons to cocrystallize is shown here to apply not only to aliphatic but also to aromatic systems. Specifically, crystallization of equimolar amounts of 1,2-bis(4-pyridyl)-ethane (**1a**) and 1,4-diiodotetrafluorobenzene (**2a**) from acetone gives the halogen-bonded infinite chains **3a** (Scheme 1a). Slow evaporation of equimolar solutions of **1a** and hydroquinone (**4a**) in the same solvent affords the hydrogen-bonded[13] 1D network **5a**. Both **3a** and **5a** precipitate as white crystals whose structures were determined by single-crystal X-ray diffraction[14] (Figure 1). The geometric parameters of the hydrogen and halogen bonds conform with values observed in similar systems.[2, 8, 10] The conformation of **1a** is different in the two cocrystals as a result of the different requirements of the intermolecular interactions acting in the two architectures, namely, the halogen and hydrogen bonds, respectively.

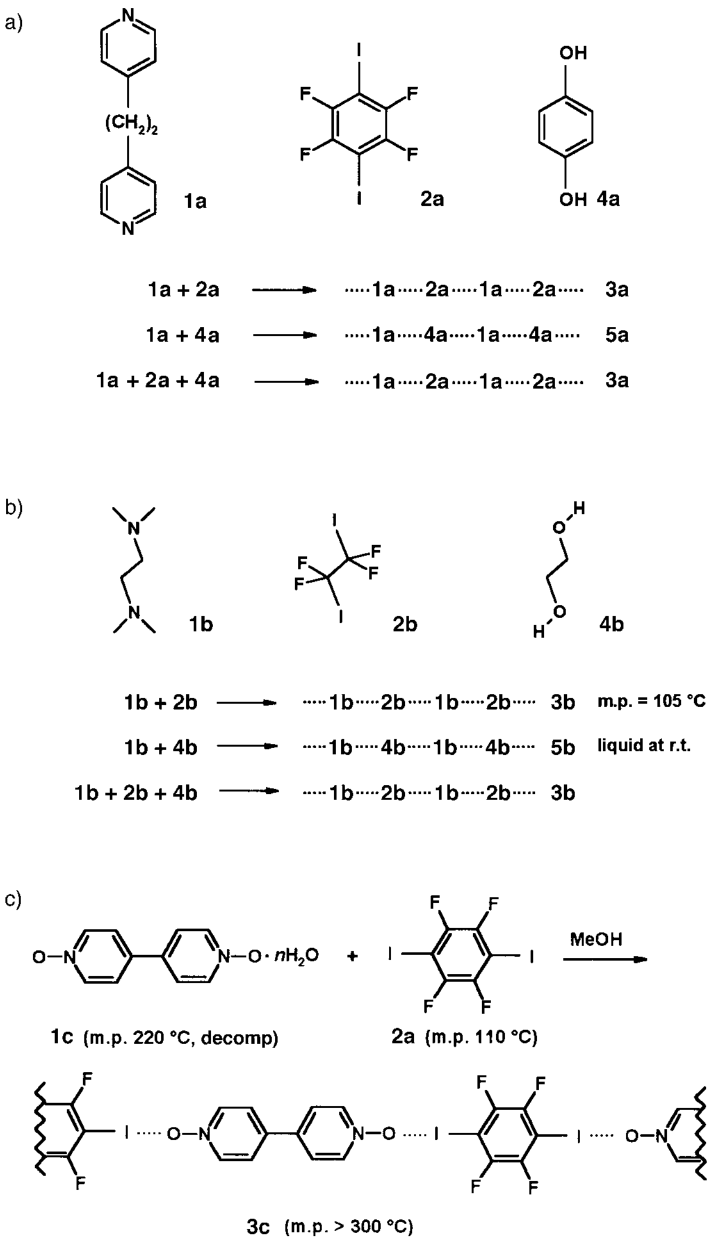

Scheme 1. Schematic diagrams representing the formation of noncovalent copolymers **3** and **5**.

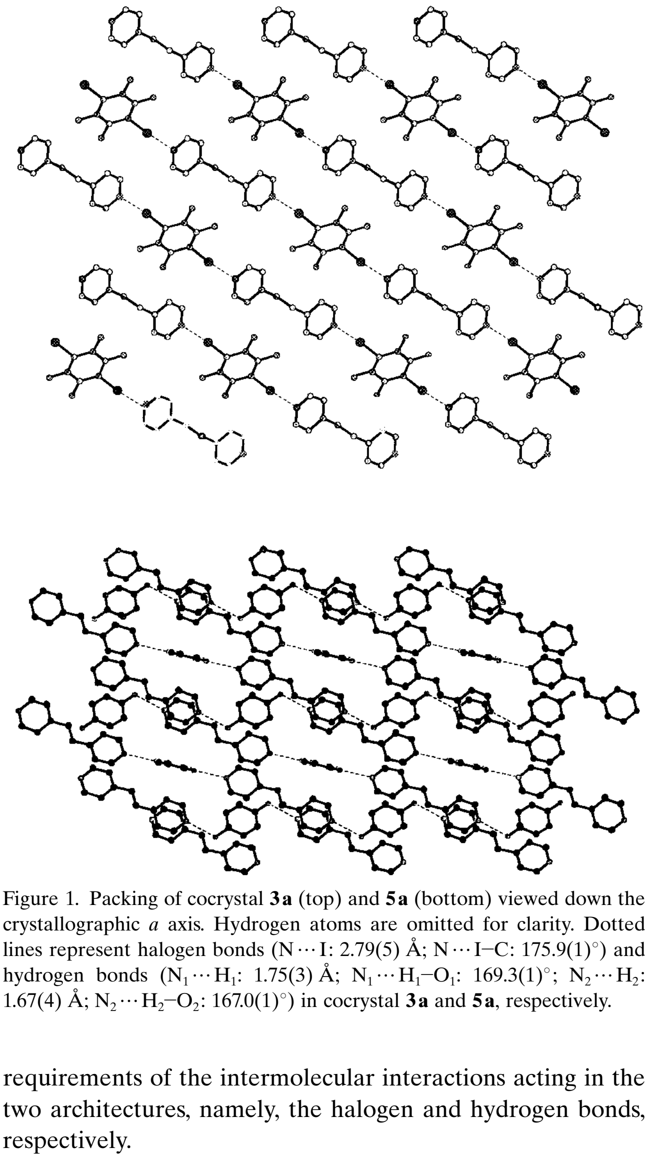

Figure 1. Packing of cocrystal **3a** (top) and **5a** (bottom) viewed down the crystallographic *a* axis. Hydrogen atoms are omitted for clarity. Dotted lines represent halogen bonds (N···I: 2.79(5) Å; N···I–C: 175.9(1)°) and hydrogen bonds ($N_1 \cdots H_1$: 1.75(3) Å; $N_1 \cdots H_1–O_1$: 169.3(1)°; $N_2 \cdots H_2$: 1.67(4) Å; $N_2 \cdots H_2–O_2$: 167.0(1)°) in cocrystal **3a** and **5a**, respectively.

In order to directly contrast hydrogen and halogen bonds, a competitive experiment was devised. Equimolar amounts of **1a**, **2a**, and **4a** were dissolved in excess acetone in a vial of clear borosilicate glass and the opened vial was closed in a cylindrical wide-mouth bottle containing vaseline oil. After a few days at room temperature cocrystal **3a**, composed of **1a** and **2a**, separated in pure form. Microanalyses, thin-layer chromatography, and NMR spectroscopic studies (^{1}H and ^{19}F nuclei) confirmed that **4a** remained in the liquid phase. Halogen bonding proves more effective than hydrogen bonding in this system in controlling the construction of programmed supramolecular architectures.

While the correlation among crystal packing, intermolecular interaction strength, and melting point cannot be quantified, the thermal characterization of compounds **1**–**5** by differential scanning calorimetry (Figure 2) nevertheless gives some useful qualitative information. The endotherms corresponding to the melting of pure components **1a** and **2a** are missing from the heating curve of cocrystal **3a**, which shows a single endotherm at higher temperature than the melting points of **1a** and **2a**. This observation indicates the formation of a new crystal species containing the two

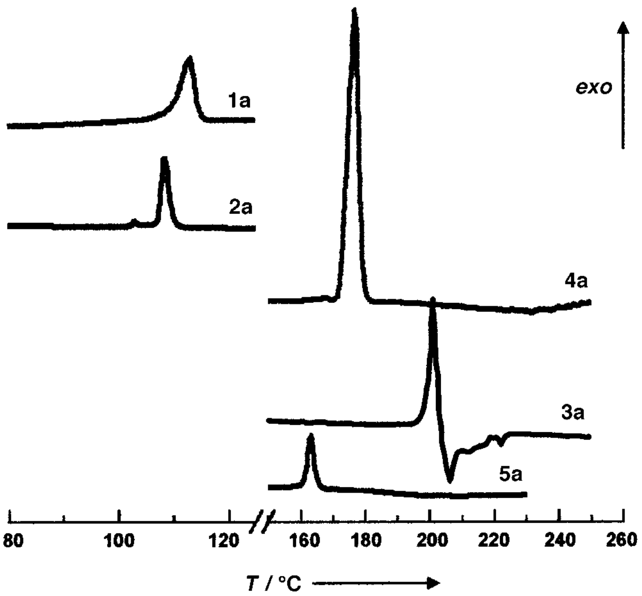

Figure 2. Heating curves (heating rate 10 °C min^{-1}) of **1a**, **2a**, **4a**, **3a**, and **5a**. The heating curve of infinite 1D network **3a** suggests the halogen bonding as a pre-reactive state[6] since the endotherm of the melting process is rapidly followed by an exothermic process.

components. Hydrogen bonding plays a major role in controlling the packing of both cocrystal **5a** and homocrystal **4a**,[15] and cocrystal **5a** melts at a lower temperature than homocrystal **4a**. In contrast, cocrystal **3a**, where the self-assembly of simple modules is mainly driven by halogen bonding, melts at a higher temperature than pure starting units **1a** ($\Delta T = \text{m.p.}_{3a} - \text{m.p.}_{1a} = 89\,^{\circ}\text{C}$) and **2a** ($\Delta T = 93\,^{\circ}\text{C}$). Cocrystal **3a** also melts at a higher temperature than cocrystal **5a** ($\Delta T = 38\,^{\circ}\text{C}$). The measurement of the enthalpies of fusion confirms the results shown by the melting temperatures and qualitatively indicates that **3a**, the assembly of which is driven by halogen bonding, is more effectively stabilized than solids held together by both weak (van der Waals forces) and strong (hydrogen-bonding) intermolecular interactions. The enthalpy of fusion of **3a** (probably underestimated as an exothermic decomposition follows the melting) is 56 kJ mol^{-1}, which is about 50 % higher than the sum of the energies of fusion of its componenets [$\Delta H_{\text{fus}}(\mathbf{1a}) + \Delta H_{\text{fus}}(\mathbf{2a})$], while $\Delta H_{\text{fus}}(\mathbf{5a})$ is 41 kJ mol^{-1}, only 10 % higher than [$\Delta H_{\text{fus}}(\mathbf{1a}) + \Delta H_{\text{fus}}(\mathbf{4a})$].

Additional competitive experiments performed with aliphatic molecular units further proved the ability of halogen bonding to prevail over hydrogen bonding in identifying the complementary motifs to be involved in the supramolecular self-assembly process. We already reported how *N,N,N′,N′*-tetramethylethylenediamine (TMEDA, **1b**) and 1,2-diiodotetrafluoroethane (**2b**), which melt at −55 and −27 °C, respectively, cocrystallize to give halogen-bonded chain **3b**, which melts at 105 °C.[10] In contrast, neat equimolar amounts of **1b** and ethylene glycol (**4b**, m.p. −13 °C) remain liquid at room temperature and solidification is observed only on cooling the mixture to −60 °C. When a stoichiometric amount of **1b** was added neat to a solution of equimolar quantities of **2b** and **4b** in chloroform, the rapid precipitation of the pure cocrystal **3b** occurred (Scheme 1b). In aqueous solution the lone pair of electrons on the nitrogen atom of **1b** is involved in the formation of hydrogen bonds with the solvent. Even under these conditions the halogen-bonding interaction is able to induce the self-assembly of single units **1b** and **2b** into infinite chain **3b**. Indeed, the cocrystal **3b** rapidly precipitated in a pure form on stirring the two-phase system of pure 1,2-diiodotetrafluoroethane (**2b**) and a 1M solution of TMEDA in water at room temperature. *N,N,N′,N′*-Tetramethyl-1,4-butanediamine as well as its -1,6-hexane- analogue and 4,4′-dipyridine behaved similarly. In all these cases halogen bonding is strong enough to drive the phasing out of different diamines from the aqueous solution, thus proving the ability of halogen bonding to also overpower hydrogen bonding in a cooperative hydrogen-bonded network.[8]

The oxygen atoms of pyridine *N*-oxide derivatives form strong hydrogen bonds as shown in the IR spectra of methanol solutions, where ν_{OH} shifts to low frequencies in the presence of pyridine-1-oxide (from 3650 to 3360 cm^{-1}). 4,4′-Dipyridyl-1,1′-dioxide is hygroscopic and usually handled in the air as the polyhydrated form 4,4′-dipyridyl-1,1′-dioxide$\cdot n\,\text{H}_2\text{O}$ (**1c**, m.p. 220 °C). When equimolar amounts of **1c** and 1,4-diiodotetrafluorobenzene (**2a**, m.p. 110 °C) are crystallized from methanol, the halogen-bonded infinite chain **3c** (m.p. > 300 °C) precipitates (Scheme 1c, see Supporting Information). Not only nitrogen atoms but also oxygen atoms can therefore form strong and selective halogen bonds that successfully rival the hydrogen bonds in controlling the self-assembly of organic compounds.

Solution calorimetry, as well as IR and NMR spectroscopy are simple and convenient tools for studying weak intermolecular interactions. Some similarities between hydrogen and halogen bonding were evident by the two spectroscopic techniques and additional information on the relative strength of the interactions was obtained by solution calorimetry. The position of ν_{OH} in IR spectra is a simple and sensitive probe to rank the strength of hydrogen bonding. Analogously, ν_{CH} of donor units **1a** and **1b** are shifted to higher frequencies in cocrystals **3a** and **3b**. Larger shifts correspond to stronger halogen bonds[16] and this is consistent with the $n \rightarrow \sigma^*$ character of the halogen bonding.[17] The difference in the chemical shift in the ^{19}F NMR spectra of *p*-fluorophenol ($\Delta\delta_{\text{F}}$) has been used as a simple, effective, and sensitive parameter to grade the involvement of the phenol oxygen atom in hydrogen-bond formation[18] and similarly the $\Delta\delta_{\text{F}}$ value in ^{19}F NMR spectra of perfluorocarbon iodides in the presence of electron donors is a sensitive parameter for probing the strength of the interaction.[4, 10, 16]

Monofunctional donor and acceptor modules were selected for solution calorimetry experiments. The 1:1 complexes formed by these units remain liquid at room temperature and by neglecting solvation effects, expected to be minor in our case,[12] the enthalpy of halogen-bond formation can be evaluated free from interferences of the enthalpy of crystallization. Specifically, when a small quantity of 1-iodoperfluorohexane was injected into a large excess of 2,2,6,6-tetramethylpiperidine (100 equiv), an exothermic effect of 31.4 kJ mol^{-1} was measured with an adiabatic accelerating rate calorimeter (ARC). This thermal effect corresponds to the enthalpy of formation of the complex (ΔH_{f}), its value is in remarkable agreement with literature data for similar interactions[19] and with quantum mechanical calculations, which yielded an interaction energy of 26 kJ mol^{-1} for $CF_3I \cdots NH_3$ in the gas phase.[20] The value for a prototype hydrogen bonding (triethylamine/*n*-butanol) was determined as $\Delta H_f = 23$ kJ mol^{-1} by using the same calorimetric technique.[21] The difference between the halogen and hydrogen bonding for other couples can be even larger than we report since the amine used by us is known to be a medium-strength electron donor.[4]

Fluorine and perfluorinated residues are strongly electron withdrawing, which promotes[22] the tendency of the iodine atoms of **2a** and **2b** to behave as electron acceptors in halogen-bonded networks. Nevertheless, halogen bonding also succeeds in driving the self-assembly of organic compounds in the absence of this promoting effect[1, 2] as formation of an electron donor–acceptor complex has been reported for several non-fluorinated iodoorganic derivatives having quite different structures.[23] Bromine atoms are less effective than iodine atoms as electron-acceptor sites, nevertheless halogen-bonded cocrystals involving bromoorganic compounds have been described.[24] Also chlorine, an even less-effective electron-acceptor atom than bromine, can be involved in halogen-bonded aggregates in the solid,[25] liquid, and gas phases.[6] Indeed, the relevance of halogen bonding in the self-assembly of structurally different molecules extends to quite different fields, spanning from biopharmacology,[26] to material science, and crystal engineering.[27] Although in the examples described here either the halogen or the hydrogen bonding drives the crystal packing and selects the molecular units assembled in the supramolecular architecture, the two interactions could also co-exist in the same crystal and cooperate in building more complex and hopefully functional[29] intermolecular structures.

Received: December 2, 1999 [Z 14347]

---

[1] O. Hassel, *Science* **1970**, *170*, 497; G. R. Desiraju, *Angew. Chem.* **1995**, *107*, 2397; *Angew. Chem. Int. Ed. Engl.* **1995**, *34*, 2311.

[2] J. M. Dumas, L. Gomel, M. Guerin, *The Chemistry of Functional Groups, Supplement D* (Eds.: S. Patai, Z. Rappoport), Wiley, New York, **1983**, p. 985; J. P. M. Lommerse, A. J. Stone, R. Taylor, F. H. Allen, *J. Am. Chem. Soc.* **1996**, *118*, 3108; H. A. Bent, *Chem. Rev.* **1968**, *68*, 587.

[3] A. Farina, S. V. Meille, M. T. Messina, P. Metrangolo, G. Resnati, G. Vecchio, *Angew. Chem.* **1999**, *111*, 2585; *Angew. Chem. Int. Ed.* **1999**, *38*, 2433.

[4] M. T. Messina, P. Metrangolo, W. Panzeri, E. Ragg, G. Resnati, *Tetrahedron Lett.* **1998**, *39*, 9069.

[5] N. F. Cheetham, A. D. E. Pullin, *Chem. Commun.* **1967**, 233.

[6] A. C. Legon, *Angew. Chem.* **1999**, *111*, 2850; *Angew. Chem. Int. Ed.* **1999**, *38*, 2687; A. C. Legon, *Chem. Eur. J.* **1998**, *4*, 1890.

[7] *Transition Metals in Supramolecolar Chemistry* (Ed.: J.-P. Sauvage), Wiley, Chichester, **1999**.

[8] G. A. Jeffrey, *An Introduction to Hydrogen Bonding*, Oxford University Press, Oxford, **1997**; O. Ermer, A. Eling, *J. Chem. Soc. Perkin Trans. 2* **1994**, 925; C. B. Aacheröy, K. R. Seddon, *Chem. Soc. Rev.* **1993**, *22*, 397.

[9] A. Manfredi, M. T. Messina, P. Metrangolo, T. Pilati, S. Quici, G. Resnati, *Supramol. Chem.*, submitted.

[10] V. Amico, S. V. Meille, E. Corradi, M. T. Messina, G. Resnati, *J. Am. Chem. Soc.* **1998**, *120*, 8261.

[11] E. Corradi, S. V. Meille, M. T. Messina, P. Metrangolo, G. Resnati, *Tetrahedron Lett.* **1999**, *40*, 7519; A. Lunghi, P. Cardillo, M. T. Messina, P. Metrangolo, W. Panzeri, G. Resnati, *J. Fluorine Chem.* **1998**, *91*, 191.

[12] Perfluorocarbon (PFC) derivatives show a unique combination of physical properties that induce a low affinity for their analogous hydrocarbon (HC) parents. Heats of solution and cohesive pressures of PFCs are quite different from those of HCs. The enthalpies of interaction between PFCs and HCs are smaller than those between HCs. Perfluorinated alkanes, ethers, and tertiary amines are practically insoluble in water and their miscibility with many organic solvents is limited. B. E. Smart in *Organofluorine Chemistry: Principles and Commercial Applications* (Eds.: R. E. Banks, B. E. Smart, J. C. Tatlow), Plenum, New York, **1994**; J. Hildebrand, D. R. F. Cochran, *J. Am. Chem. Soc.* **1949**, *71*, 22; D. L. Dorset, *Macromolecules* **1990**, *23*, 894.

[13] T. Koyama, A. Wakisaka, *J. Chem. Soc. Faraday Trans.* **1997**, *93*, 3813.

[14] Precipitation of cocrystals **3a–c** and **5a** occurs from solutions that are quite far from saturation in the single components **1a–c** and **2a**. This observation further proves the ability of halogen bonding to overcome hydrogen bonding and other intermolecular interactions to drive the formation of a crystalline solid. In cocrystal **3a**, the aromatic rings stack parallel to each other, about 5 Å apart, forming distinct columns of perfluorinated and hydrocarbon compounds. This arrangement is probably imposed by van der Waals interactions involving iodine atoms and the 1,2-bis(4-pyridyl)ethane molecules. On the contrary, in cocrystal **5a**, the columnar structure is absent and the hydroquinone units are arranged in a herringbone way, where the aromatic rings are tilted by about 60° with respect to each other. Data were collected for both **3a** and **5a** using $\lambda_{CuK\alpha} = 1.54178$ Å, $\theta/2\theta$ scan mode ($3.5 \leq \theta \leq 70.0^\circ$, at 293(2) K and corrected for Lorentz, polarization and absorption; both structures were solved by direct methods using SIR97 and refined using SHELX97 against F^2, with hydrogen atoms at calculated positions in the riding mode. Crystal data are as follows: cocrystal **3a**: $0.65 \times 0.50 \times 0.35$ mm^3, triclinic, space group $P\bar{1}$, $a = 5.032(2)$, $b = 9.902(4)$, $c = 10.598(5)$ Å, $\alpha = 64.70(3)$, $\beta = 82.24(4)$, $\gamma = 87.94(4)^\circ$; $V = 472.9(5)$ Å^3; $Z = 1$; $\rho_{calcd} = 2.058$ g cm^{-3}, $\mu = 26.5$ mm^{-1}; 2151 collected reflections, 1588 independent, 119 refined parameters, $R_1 = 0.067$ (for 1573 data with $I \geq 2\sigma(I)$). Cocrystal **5a**: $0.55 \times 0.40 \times 0.35$ mm^3, triclinic, space group $P\bar{1}$, $a = 7.458(1)$, $b = 9.424(1)$, $c = 11.804(1)$ Å, $\alpha = 95.234(6)$, $\beta = 93.023(2)$, $\gamma = 108.338(8)^\circ$; $V = 781.3(1)$ Å^3; $Z = 2$; $\rho_{calcd} = 1.251$ g cm^{-3}, $\mu = 0.66$ mm^{-1}; 5168 collected reflections, 2737 independent, 208 refined parameters $R_1 = 0.060$ (for 1604 data with $I \geq 2\sigma(I)$). Crystallographic data (excluding structure factors) for the structures reported in this paper have been deposited with the Cambridge Crystallographic Data Centre as supplementary publication nos. CCDC-137462 **3a** and -137463 for **5a**. Copies of the data can be obtained free of charge on application to CCDC, 12 Union Road, Cambridge CB2 1EZ, UK (fax: (+44) 1223-336-033; e-mail: deposit@ccdc.cam.ac.uk).

[15] K. Maartmen-Moe, *Acta Crystallogr.* **1966**, *21*, 979.

[16] "Asymmetric Fluoroorganic Chemistry: Synthesis, Applications and Future Directions": M. T. Messina, P. Metrangolo, G. Resnati, *ACS Symp. Ser.* **1999**, *746*.

[17] R. Foster, *Organic Charge-Transfer Complexes*, Academic Press, London, **1969**, p. 100.

[18] D. Gurka, R. W. Taft, *J. Am. Chem. Soc.* **1969**, *91*, 4794.

[19] D. W. Larsen, A. L. Allred, *J. Phys. Chem.* **1965**, *69*, 2400.

[20] S. V. Meille, P. Metrangolo, G. Raos, G. Resnati, G. Valerio, *J. Phys. Chem. A*, in press.

[21] E. M. Arnett, L. Joris, E. Mitchell, T. S. S. R. Murty, T. M. Gorrie, P. Von R. Schleyer, *J. Am. Chem. Soc.* **1970**, *92*, 2365.

[22] R. Weiss, O. Schwab, F. Hampel, *Chem. Eur. J.* **1999**, *5*, 968.

[23] A. Ranganathan, V. R. Pedireddi, *Tetrahedron Lett.* **1998**, *39*, 1803; R. Weiss, M. Rechinger, F. Hampel, A. Wolski, *Angew. Chem.* **1995**, *107*, 483; *Angew. Chem. Int. Ed. Engl.* **1995**, *34*, 441; J. A. R. P. Sarma, F. H. Allen, V. J. Hoy, J. A. K. Howard, R. Thaimattam, K. Biradha, G. R. Desiraju, *Chem. Commun.* **1997**, 101.

[24] J. P. Lorand, *Tetrahedron Lett.* **1971**, 2511.

[25] K. Xu, M. Ho, R. A. Pascal, Jr., *J. Am. Chem. Soc.* **1994**, *116*, 105.

[26] L. K. Steinrauf, J. A. Hamilton, B. C. Braden, J. R. Murrel, M. D. Benson, *J. Biol. Chem.* **1993**, *268*, 2425.
[27] G. R. Desiraju, *Crystal Engineering: The Design of Organic Solids*, Elsevier, Amsterdam, **1989**.
[28] J.-M. Lehn, *Supramolecular Chemistry: Concepts and Perspectives*, VCH, Weinheim, **1995**.

Spin-Density Map of the Triplet Ground State of a Titanium(IV) Complex with Schiff-Base Diquinone Radical Ligands: An Investigation Using Polarized-Neutron Diffraction and Density-Functional Theory**

Yves Pontillon, Alessandro Bencini, Andrea Caneschi, Andrea Dei, Dante Gatteschi,* Béatrice Gillon,* Claudio Sangregorio, John Stride, and Federico Totti

During the last decade, the design of new molecular ferromagnets has been a field of growing interest.[1] Ferromagnetic interactions between organic radicals, although rare, are now recognized as real.[2–5] The final goal of obtaining molecular-based ferromagnets may be achieved if, for example, the individual building blocks carrying unpaired electrons are arranged such that the magnetic orbitals remain orthogonal to each other.[6] With this in mind, attempts have been made to use organic radicals bound to diamagnetic metal ions and some elegant examples of moderate ferromagnetic coupling have been reported.[7] In particular, a titanium(IV) complex TiL$_2$, where L is the dianion of the radical ligand 3,5-di-*tert*-butyl-1,2-semiquinonato-1-(2-hydroxy-3,5-di-*tert*-butylphenyl)imine, has been found to be characterized by a triplet ground state arising from a ferromagnetic interaction ($J = 56\,\text{cm}^{-1}$) between the two ½-spin coordinated radical ligands.[8] This compound crystallizes in the triclinic $P\bar{1}$ space group. The metal ion is octahedrally coordinated by the two ligands, which occupy the meridional sites of the coordination polyhedron (Figure 1). The two ligands are orthogonal to each other and the dihedral angles between the aromatic rings in the two ligands are 9.7° and 5.4°, respectively.

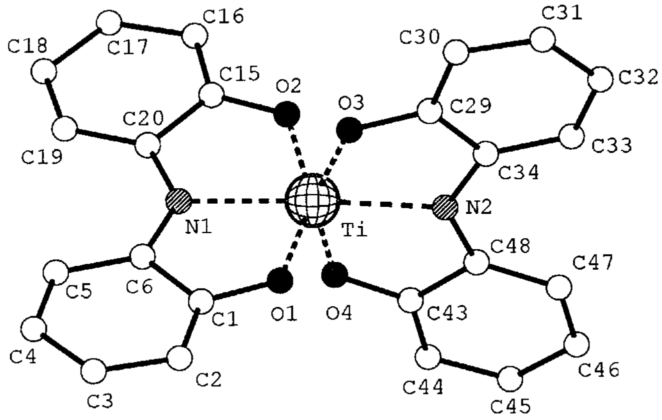

Figure 1. View of the TiL$_2$ molecule showing the numbering of the atoms. The *tert*-butyl groups are omitted for clarity.

It has been proposed[8] that the triplet ground state is stabilized by the topological degeneracy of the two magnetic orbitals of the ligands. Assuming an overall C_{2v} symmetry for the complex, the two π^* magnetic orbitals span the b_1 and b_2 irreducible representations and are, therefore, orthogonal to each other and this provides a rationalization of the observed ferromagnetic coupling.

The exchange interactions between the two radicals may arise from both direct overlap between the ligand magnetic orbitals (the shortest interligand oxygen–oxygen distances are about 2.7 Å) and superexchange as mediated by metal orbitals.[8, 9] In the former case, the unpaired spin density (SD) is expected to be located onto the ligands, whereas in the latter a sizeable SD must be observed also on the metal ion, which, according to the formal Ti^{+4} charge, has a d^0 configuration.

In this communication, we report the preliminary results concerning a polarized neutron diffraction (PND) study of the TiL$_2$ compound. The PND technique is well adapted for measuring the spin-density distribution in magnetic crystalline molecular compounds.[10, 11] It is applicable to single crystals in which the spin density has been partly or totally aligned by an external magnetic field.

The PND experiment was performed on the polarized-neutron lifting-counter diffractometer 5c1 at the Orphee reactor (CEA-Saclay, France). A small TiL$_2$ crystal, $2 \times 2 \times 1\,\text{mm}^3$, was mounted with the *a* axis parallel to the 7 T applied magnetic field. The flipping ratios (F_N) of the more intense reflections were measured: $F_N = 39{:}1$ at $T = 1.5$ K. By measuring the integrated nuclear intensities of the same set of reflections in a zero field,[12] it was found that the room temperature X-ray crystal structure[8] could be used to model and normalize the F_N and to determine their phase. The magnetic structure factors (F_M) were obtained through standard techniques.[12]

There are different possible approaches to analyze the PND experimental data.[11] A versatile method is based on the modeling of the spin-density distribution $s(r)$ followed by a direct expansion of the spin density around the nuclei. This

---

[*] D. Gatteschi, Y. Pontillon,[+] A. Bencini, A. Caneschi, A. Dei,
C. Sangregorio, F. Totti,
Dipartimento di Chimica
Università degli Studi di Firenze
Via Maragliano 77, 50144 Florence (Italy)
Fax: (+39) 055-35-48-45
E-mail: gattesch@blu.chim1.unifi.it

B. Gillon, J. Stride
CEA Saclay
Laboratoire Léon Brillouin
91191 Gif-sur-Yvette Cedex (France)
Fax: (+33) 01-69-08-82-61
E-mail: gillon@bali.saclay.cea.fr

[+] Present address:
Institut Laue Langevin
6 rue J. Horowitz
BP 156, 38042 Grenoble Cedex 9 (France)

[**] This work was supported by the 3MD EU network (contract ERB 4061 PL 97-0197).